ROYAL SOCIETY OF CHEMISTRY

COMMUNICATION

CrossMark
click for updates

CO₂-switchable poly (N-isopropylacrylamide) microgel-based etalons†

Qiang Matthew Zhang, Andrews Ahiabu, Yongfeng Gao and Michael J. Serpe*

A series of pyridine-functionalized poly (N-isopropylacrylamide)-based microgels were synthesized. Subsequently, a structured photonic device was fabricated by sandwiching the microgels between two thin Au layers, and their response to CO_2 investigated. We show that devices show an optical response to CO_2, which is reversible over many cycles.

Smart materials that can adapt and actuate in response to environmental or external stimuli have attracted much scientific interest in the past decades.[1–4] Specifically, polymeric smart materials that are able to swell, shrink or bend in response to environmental stimuli are finding uses in fields ranging from medicine to materials science and physics.[5,6] The external stimuli can be: light,[7,8] temperature,[9,10] magnetic field,[11] mechanical forces.[12] Additionally, materials can respond to changes in the conditions of the solution the material is exposed to, such as pH,[13,14] or the presence of biomolecules.[15]

Carbon dioxide (CO_2), plays a key role in biological systems in the environment. For example, CO_2 can stabilize intracellular pH through a series of equilibrium reactions, see eqn (1).

$$CO_2 + H_2O \rightarrow H_2CO_3 \rightarrow H^+ + HCO_3^- \qquad (1)$$
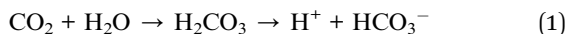
Additionally, high/low CO_2 levels can lead to certain metabolism-related diseases.[16] Recently, CO_2 has emerged as a new species that can induce changes in material properties. This has become possible after the early work of the Jessop group,[17] who demonstrated that long chain alkyl amidine compounds are able to be reversibly transformed into charged surfactants, merely by passing CO_2 through them. In this way, the emulsions are stabilized and can be destabilized by bubbling N_2, Ar, or air through the amidinium bicarbonate solution. Polymeric vesicles formed by the self-assembly of

amidino containing block copolymers have been reported, which can reversibly respond to CO_2.[18,19] The size of these vesicles can be reversibly tuned over a wide range by the addition of CO_2 and Ar to cause the smart expansion and contraction cycles, respectively. In another example, the size, shape, and morphology of polymer assemblies can be modulated by controlling the CO_2 stimulation levels.[20] However, up to now, CO_2-responsive system is still rarely investigated.

Our group's research mainly focuses on microgels, which are colloidal hydrogel particles with diameters that range from several hundreds of nanometers to a few microns.[27,28] Previously, our group has developed responsive microgels-based devices for applications as: sensors, artificial muscles and drug delivery motifs.[21–27] In the present work, CO_2-responsive microgels were prepared by incorporating pyridine into poly-(N-isopropylacrylamide) (pNIPAm)-based microgels. It can transform into a positive charged pyridinium species upon reaction with H_2CO_3, and the microgels expand due to the electrostatic repulsion of pyridinium species. The response is similar with the amidine[18,19] and amine[28] systems.

In this study, we show that optical devices capable of detecting CO_2 can be fabricated. The fabrication of the optical devices has been detailed previously,[29] and is shown in Fig. 1.
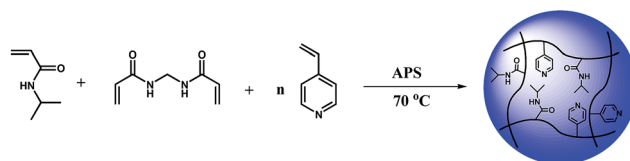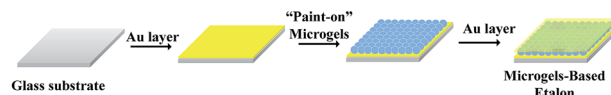

Fig. 1 (a) Microgel synthesis scheme, and (b) etalon fabrication process.

Department of Chemistry, University of Alberta, Edmonton, Alberta, Canada. E-mail: michael.serpe@ualberta.ca; Fax: +1 780 492 8231; Tel: +1 780 492 5778

Briefly, a glass substrate was coated with 2 nm Cr and 15 nm Au, and pNIPAm-*co*-4VP microgels "painted" on top.[23] After rinsing away the microgels not directly bound to the Au layer, another 2 nm Cr and 15 nm Au layer was deposited on the microgels to form a sandwich structure, which is referred to as an etalon. This structure exhibits color, and multipeak reflectance spectra; the position of the peaks in the reflectance spectra can be predicted using eqn (2):

$$\lambda m = 2nd \cos \theta \qquad (2)$$

where λ is the wavelength maximum of the peak (s), m is the peak order, n is the refractive index of the dielectric, d is the spacing between the mirrors, and θ is the angle of incidence. The position of the peaks in the reflectance spectra depends on the distance between two Au layers and the refractive index of microgel. Since the microgel solvation state can be modulated with environmental change, the response of microgels to the environmental stimulant can be observed as a shift in the position of the reflectance peaks.

Pyridine-containing pNIPAm-based microgels were synthesized *via* the copolymerization of 4-vinyl pyridine, *N*-isopropylacrylamide (NIPAm) and *N*,*N*′-methylenebis(acrylamide) (BIS) (see ESI†). The microgels are denoted as MG-X%, where X represents the percent of pyridine, from 15% to 25%. Transmission electron microscope (TEM) images of the as synthesized microgels are shown in Fig. 2. As can be seen, in both cases, the microgels are spherical, with dry diameters in the range of 1.5–2.5 μm (*via* analysis of the microscope images). The apparent hydrodynamic diameters of microgels were also characterized by dynamic light scattering (DLS) (Fig. S1 and S2†). MG-15%, MG-20% and MG-25% exhibit a hydrodynamic radius (R_h) of 2049 nm, 2254 nm, and 2343 nm in deionized (DI) water at 30 °C, respectively. The microgels also showed a lower critical solution temperature (LCST) of around 32 °C in DI water. The ability of the microgels in solution to swell as a function of pH and pyridine content was also investigated, and they showed the expected increase in diameter as solution pH was decreased. These data are shown in ESI.† This is a direct result of pyridine protonation.

Microgel-based etalons were subsequently constructed from the synthesized microgels, and their responsivity to stimuli was investigated. To confirm the basic responsivity and function of the etalons, initial experiments focused on characterizing the etalon thermoresponsivity. MG-25% microgels were used to
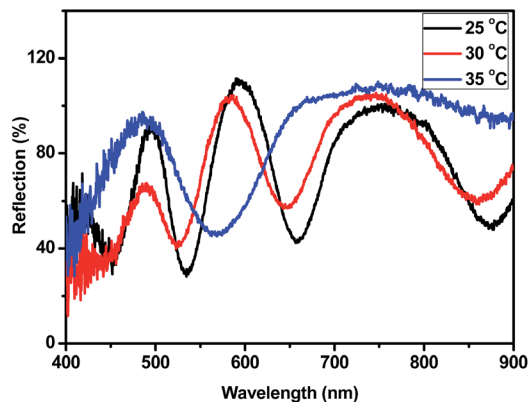

Fig. 3 Reflectance spectra for a MG-25% etalon in water at the indicated temperatures.

make etalons, which were immersed in water (~neutral pH); the resulting reflectance spectrum is shown in Fig. 3. As can be seen, a characteristic multipeak reflectance spectrum was observed, with peaks at 501 nm, 595 nm, and 760 nm at 30 °C. From the relative positions of the reflectance peaks, and using eqn (1), the order (m) of each peak can be calculated. The peak at 501 nm is $m = 6$ (noted as λ_6), λ_5 is 595 nm, λ_4 is 760 nm. When conducting these experiments, it is important to compare the same order peaks before and after introduction of a stimulus. When the temperature was increased from 25 to 35 °C, λ_5 exhibited a blue shift of 89 nm, while it exhibits an additional ~25 nm shift (114 nm total shift) when the temperature was increased to 45 °C (Fig. S3†). All etalons exhibit similar thermoresponsivity (Fig. S3†). The peak shifts are a direct result of the thermoresponsivity of the pNIPAm-based microgels, which collapse at elevated temperature, decreasing the distance between the etalons two gold mirrors. The blue shifts can be predicted from eqn (2).[30,31]

Since the basic thermal response of the pNIPAm microgel-based devices was investigated, the etalons response to CO_2 was subsequently characterized in DI water. During this process, CO_2 gas was bubbled into DI water, which causes the pH decrease from 6.8 to 3.8. Fig. 4 (a) shows a representative reflectance spectrum for a device fabricated from MG-25%, and a series of reflectance spectra after CO_2 exposure. As can be seen, CO_2 exposure causes a 35 nm red shift in the position of the reflectance peak (λ_5) after CO_2 exposure for the indicated times. The reflectance spectrum is fully stabilized within 90 min, although a significant response is noted within 40 min. We propose that this red shift is a result of positive charged pyridinium generation in the microgel from the reaction of pyridine group and carbonic acid. This ionization increases the microgel's hydrophilicity and generates Coulombic repulsion between microgel pyridinium groups, which lead to swelling of the microgels, increasing the distance between the mirrors. We note that these experiments were conducted at 30 °C. We found that temperature variations could change the extent of the response, 30 °C gave us the best response presumably due to the favorable hydrophilic/hydrophobic interactions, combined with the microgel diameter at this temperature allowing for maximal
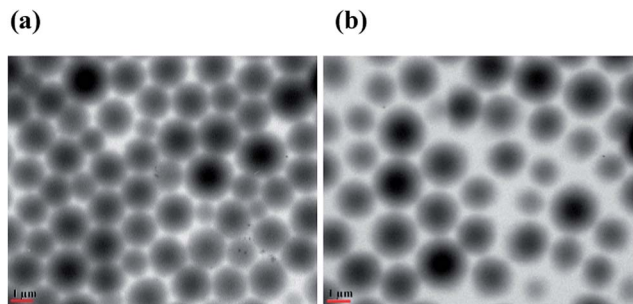

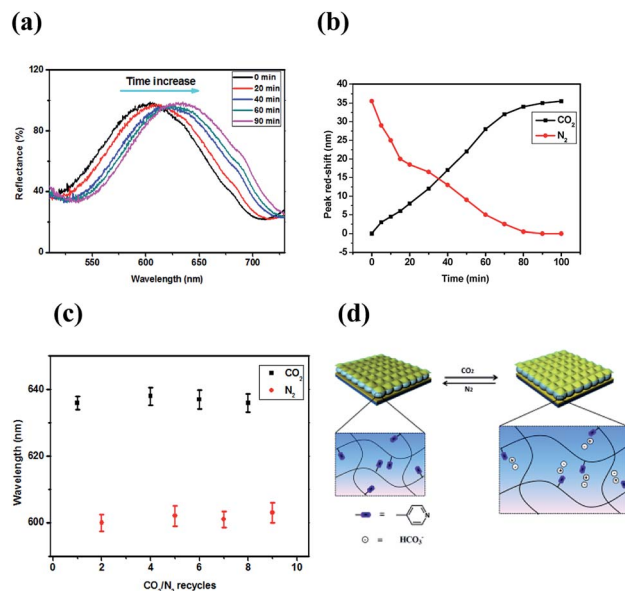Fig. 2 TEM micrographs of (a) MG-25%, and (b) MG-15%.

496 | *J. Mater. Chem. C*, 2015, **3**, 495–498

This journal is © The Royal Society of Chemistry 2015

Fig. 4 (a) Reflectance spectra (λ_5) for a MG-25% etalon exposed to CO_2 for the indicated times; (b) peak shift (λ_5) for a MG-25% etalon exposed to N_2 and CO_2 for the indicated times in water at 30 °C; (c) λ_5 peak wavelength for MG-25% etalon as a function of CO_2/N_2 cycle number. Three different devices were tested, and one of them was shown in (a) and (b). (c) Each point is the average from three different devices, while the error bars indicate standard deviation. (d) Response mechanism of etalon. The rate of gas flow was 5 mL min^{-1}.

microgel size change upon pyridine ionization (Fig. S5†). We also point out that the extent of the peak shifts increases with the amount of pyridine in the microgels – 22 nm (MG-15%), 28 nm (MG-20%), and 35 nm (MG-25%) (Fig. S5†). For comparison, the pH responsivity of etalon (MG-25%) was also tested, and the result was shown in Fig. S6.† It exhibited red-shift of 41 nm, which is slightly higher than that triggered by CO_2 (35 nm). This may be due to the enhanced hydrophilicity of Cl$^-$ compared to HCO_3^-. The kinetics of the peak shift can be seen in Fig. S7.† As can be seen, while the pH changes quickly and stabilizes within 20 min, the etalon takes 90 min to fully stabilize.

It is worth noting that by passing N_2 through the solution to remove CO_2 the solution pH increases from 3.8 to 6.8; the etalon's reflectance spectrum blue shifts and ultimately returns to its initial state as a result (Fig. 4b). This is due to the pH increase neutralizing the pyridinium groups to the uncharged pyridine, and the microgels deswell as a result. According to eqn (2), a blue-shift of the peaks in the reflectance spectrum was predicted. As can be seen in Fig. 4c, the reversibility in the etalons response is robust over at least 4 CO_2/N_2 cycles. The entire process can be viewed as a microgel "breathing" process, as shown in Fig. 4d, similar to volume self-adjustment by organelles.[32]

In summary, pyridine-containing microgels were synthesized, and used to fabricate CO_2 responsive microgel-based etalons. The resultant etalons were shown to exhibit both temperature and CO_2 responsivity. The extent of the response could be controlled in a systematic fashion by varying the microgel's pyridine concentration. We also showed that the

etalon's response could be reversed by bubbling N_2 gas through the solution, and the etalons response can be varied over multiple cycles without a significant loss in responsivity. Due to their low cost ~0.04 CAD/square inch and ease of use, we feel that these devices could find many uses in the real world. For example, it is well known that ocean acidification is caused by an increase in the concentration of CO_2 in air.[33] Therefore, since CO_2 is responsible for the acidification; our devices could be used to report on CO_2 concentration in air.

Acknowledgements

Notes and references

1 L. Zhai, *Chem. Soc. Rev.*, 2013, **42**, 7148–7160.
2 M. F. Maitz, U. Freudenberg, M. V. Tsurkan, M. Fischer, T. Beyrich and C. Werner, *Nat. Commun.*, 2013, **4**, 2168.
3 M. A. C. Stuart, W. T. S. Huck, J. Genzer, M. Muller, C. Ober, M. Stamm, G. B. Sukhorukov, I. Szleifer, V. V. Tsukruk, M. Urban, F. Winnik, S. Zauscher, I. Luzinov and S. Minko, *Nat. Mater.*, 2010, **9**, 101–113.
4 C. Weder, *Nature*, 2009, **459**, 45–46.
5 H. Therien-Aubin, Z. L. Wu, Z. H. Nie and E. Kumacheva, *J. Am. Chem. Soc.*, 2013, **135**, 4834–4839.
6 G. Q. Pan, Q. P. Guo, Y. Ma, H. L. Yang and B. Li, *Angew. Chem., Int. Ed.*, 2013, **52**, 6907–6911.
7 J. Liu, S. Wen, Y. Hou, F. Zuo, G. J. Beran and P. Feng, *Angew. Chem.*, 2013, **125**, 3323–3327.
8 R. Asai, H. Nemoto, Q. Jia, K. Saito, A. Iwase and A. Kudo, *Chem. Commun.*, 2014, **50**, 2543–2546.
9 Z. Yu, N. Li, P. Zheng, W. Pan and B. Tang, *Chem. Commun.*, 2014, **50**, 3494–3497.
10 J. Zhu, Y. Zhang, D. Lu, R. N. Zare, J. Ge and Z. Liu, *Chem. Commun.*, 2013, **49**, 6090–6092.
11 S. Y. Lee and S. Yang, *Angew. Chem., Int. Ed.*, 2013, **52**, 8160–8164.
12 Y. Chen, A. Spiering, S. Karthikeyan, G. W. Peters, E. Meijer and R. P. Sijbesma, *Nat. Chem.*, 2012, **4**, 559–562.
13 G. H. Hwang, K. H. Min, H. J. Lee, H. Y. Nam, G. H. Choi, B. J. Kim, S. Y. Jeong and S. C. Lee, *Chem. Commun.*, 2014, **50**, 4351–4353.
14 B. Wang and Z. Guo, *Chem. Commun.*, 2013, **49**, 9416–9418.
15 S. Wu, X. Huang and X. Du, *Angew. Chem.*, 2013, **125**, 5690–5694.
16 N. M. Dixon and D. B. Kell, *J. Appl. Microbiol.*, 1989, **67**, 109–136.

This journal is © The Royal Society of Chemistry 2015

J. Mater. Chem. C, 2015, **3**, 495–498 | **497**

17 Y. Liu, P. G. Jessop, M. Cunningham, C. A. Eckert and C. L. Liotta, *Science*, 2006, **313**, 958–960.

18 Q. Yan, J. Wang, Y. Yin and J. Yuan, *Angew. Chem., Int. Ed.*, 2013, **52**, 5070–5073.

19 Q. Yan, R. Zhou, C. Fu, H. Zhang, Y. Yin and J. Yuan, *Angew. Chem.*, 2011, **123**, 5025–5029.

20 Q. Yan and Y. Zhao, *J. Am. Chem. Soc.*, 2013, **135**, 16300–16303.

21 M. R. Islam, X. Li, K. Smyth and M. J. Serpe, *Angew. Chem., Int. Ed.*, 2013, **52**, 10330–10333.

22 Y. Gao, G. P. Zago, Z. Jia and M. J. Serpe, *ACS Appl. Mater. Interfaces*, 2013, **19**, 9803–9808.

23 C. D. Sorrell and M. J. Serpe, *Adv. Mater.*, 2011, **23**, 4088–4092.

24 C. D. Sorrell, M. C. Carter and M. J. Serpe, *Adv. Funct. Mater.*, 2011, **21**, 425–433.

25 M. R. Islam and M. J. Serpe, *Chem. Commun.*, 2013, **49**, 2646–2648.

26 Q. M. Zhang, W. Xu and M. J. Serpe, *Angew. Chem., Int. Ed.*, 2014, **53**, 4827–4831.

27 X. Li and M. J. Serpe, *Adv. Funct. Mater.*, 2014, **24**, 4119–4126.

28 X. Su, T. Robert, S. M. Mercer, C. Humphries, M. F. Cunningham and P. G. Jessop, *Chem.–Eur. J.*, 2013, **19**, 5595–5601.

29 Q. M. Zhang, X. Li, M. R. Islam, M. Wei and M. J. Serpe, *J. Mater. Chem. C*, 2014, **2**, 6961–6965.

30 S. Seiffert, *Angew. Chem., Int. Ed.*, 2013, **52**, 11462–11468.

31 S. Nayak and L. A. Lyon, *Chem. Mater.*, 2004, **16**, 2623–2627.

32 R. Heald and O. Cohen-Fix, *Curr. Opin. Cell Biol.*, 2014, **26**, 79–86.

33 K. Caldeira and M. E. Wickett, *Nature*, 2003, **425**, 365.

498 | *J. Mater. Chem. C*, 2015, **3**, 495–498

This journal is © The Royal Society of Chemistry 2015